Available online at www.sciencedirect.com
SCIENCE DIRECT®
Journal of Sound and Vibration 286 (2005) 941–961
JOURNAL OF SOUND AND VIBRATION
www.elsevier.com/locate/jsvi

Shape optimization on constrained single-layer sound absorber by using GA method and mathematical gradient methods

Ying-Chun Chang*, Long-Jyi Yeh, Min-Chie Chiu, Gaung-Jer Lai

Department of Mechanical Engineering, Tatung University, 40 Chungshan N. Rd, 3rd Sec, Taipei, 104, Taiwan, ROC

Received 22 August 2003; received in revised form 21 May 2004; accepted 25 October 2004
Available online 5 January 2005

Abstract

The problem of space constraint in sound absorber design occasionally occurs in practical design work for the requisite maintenance and access. To ultimate the performance of sound absorption under space constraint, the shape optimization to maximize the absorber's performance is thus arising, accordingly. In this paper, the numerical optimal studies on single-layer sound absorber are presented.

Two categories of numerical approaches, including the genetic algorithm (*GA*) method and traditional gradient methods, are applied into the muffler design work. The acoustic impedance of sound absorber in evaluating the sound absorption coefficient is in conjunction with these numerical techniques. Here, *GA* technique and traditional gradient methods are programmed by *MATLAB* and *FORTRAN* individually. A numerical case on the single-layer sound absorber in dealing with the pure tone noise is introduced. Before optimization, one example is tested and compared with the experimental data for an accuracy check of the mathematical model. It indicates that the result is in good agreements. Consequently, the novel scheme, genetic algorithm, is capable of solving the shape optimization of a single-layer sound absorber under boundary constraint.

*Corresponding author.
E-mail addresses: ycchang@ttu.edu.tw (Y.-C. Chang), ljyeh@ttu.edu.tw (L.-J. Yeh), min-chie.chiu@ctci.com.tw (M.-C. Chiu).

0022-460X/$ - see front matter © 2004 Elsevier Ltd. All rights reserved.
doi:10.1016/j.jsv.2004.10.039

Nomenclature

j	$\sqrt{-1}$
bit_no	bit length
c_0	sound speed ($m\,s^{-1}$)
d	diameter of perforated hole on the front plate (m)
D_0	thickness of absorber (m)
D_f	thickness of acoustic fiber (m)
elit	selection of elite (1 for yes and 0 for no)
f	cyclic frequency (Hz)
gen_no	maximum no. of generation
k	wavenumber
k_{fiber}	complex propagation constant of acoustic fiber
k_1	real part of complex k_{fiber}
k_2	imaginary part of complex k_{fiber}
L	air depth of sound absorber (m)
$p\%$	porosity of the perforated plate ($= \varepsilon^* 100\%$) (%)
p_i	acoustic pressure at point i (Pa)
pc	crossover ratio
pm	mutation ratio
popuSize	no. of population
q	thickness of the perforated plate (m)
R	acoustic flow resistance of acoustic fiber (MKS rayls m^{-1})
R_{fiber}	real part of complex Z_{fiber}
r_p	penalty factor
r'_p	penalty factor
u_i	acoustic particle velocity at point i ($kg\,s^{-1}$)
X_{fiber}	imaginary part of complex Z_{fiber}
Z_i	specific normal impedance at point i
Z_{fiber}	characteristic impedance of acoustic fiber
α	sound absorption coefficient of absorber
ρ_0	air density ($kg\,m^{-3}$)
ω	angular frequency ($rad\,s^{-1}$)
ν	kinematic viscosity of air ($= 15 \times 10^{-6}\,m^2/s$)
ε	porosity of the perforated plate
δ	viscous boundary layer thickness of the perforated plate (m)
Φ	modified objective function

1. Introduction

The trial and error method in the enhancement of the sound absorber design is considered tedious and expensive, and the thickness of the absorber is often limited for the demand of maintenance and access. Many researches of the sound absorber were well developed; however, the discussion of sensitivity between design parameters under space constraints is rarely accomplished. Therefore, the interest to optimize sound absorption of the absorber under space constraints is increasing in the field.

To solve the optimal design of the sound absorber, two categories of numerical assessments are used. One is the classical gradient method, including the (1) exterior penalty function (*EPFM*), (2) interior penalty function method (*IPFM*) and (3) feasible direction method (*FDM*) [1–3]. The other is the genetic algorithm which has been applied successfully in many fields of optimization problems [4].

In this paper, a numerical case of eliminating the pure tone noise by a single-layer sound absorber is also fully illustrated. The formula of transfer matrix for isotropic and homogeneous material [5–7] is applied. In addition, the continuity of the particle velocity is also applied in the derivation of the perforated plate [7–9]. Moreover, the semi-empirical formula of specific normal impedance of acoustic fiber by Delany and Bazley [10] as well as that of the perforated plate by Beranek and Ver [11] is in conjunction with the numerical methods for optimization.

Unlike the traditional work by the trial and error method, which is considered tedious and expensive, this paper surely provides quick and effective ways for the enhancement of the single-layer sound absorber by optimal simulation.

2. Theoretical background

For a 3D acoustic wave propagating through a quiescent medium, which is homogeneous and isotropic (with the rectangular partitions as shown in Fig. 1 with b length and h width), the wave governing equation is [8]

$$\left(\frac{\partial^2}{\partial t^2} - c_0^2\nabla^2\right)p = 0. \tag{1}$$

By using the separation of variable method, the equation yields

$$p(x,y,z,t) = \sum_{m=0}^{\infty}\sum_{n=0}^{\infty}\cos\frac{m\pi x}{b}\cos\frac{n\pi y}{h}(C_{1,m,n}e^{-jk_{z,m,n}z} + C_{2,m,n}e^{+jk_{z,m,n}z})e^{jwt}, \tag{2}$$

$$u_z(x,y,z,t) = \frac{1}{\rho_0 c_0 k_0}\sum_{m=0}^{\infty}\sum_{n=0}^{\infty}k_{z,m,n}\cos\frac{m\pi x}{b}\sin\frac{n\pi y}{h}(C_{1,m,n}e^{-jk_{z,m,n}z} + C_{2,m,n}e^{+jk_{z,m,n}z})e^{jwt} \tag{3}$$

with the compatibility condition

$$k_{x,m}^2 + k_{y,n}^2 + k_{z,m,n}^2 = k_0^2 \tag{4a}$$

or

$$k_{z,m,n}^2 = k_0^2 - \left(\frac{m\pi}{b}\right)^2 - \left(\frac{n\pi}{h}\right)^2. \tag{4b}$$

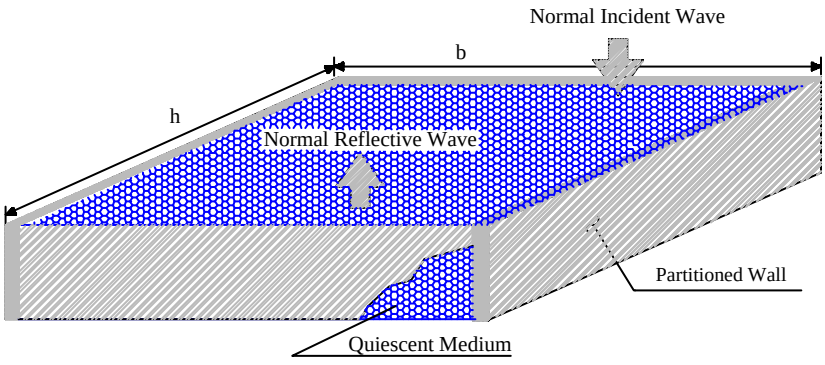

Fig. 1. 3D wave propagating through a partitioned porous material.

Consequently, only the plane wave at the fundamental mode of ($m = 0$, $n = 0$) will propagate if the frequency is small enough so that

$$f < \frac{c_0}{2h}, \tag{5}$$

where h is the larger value of the transverse dimensions of the rectangular partition.

For a 1D plane wave propagating perpendicularly through a partitioned and uniform section, the acoustic pressure is reduced to

$$p(z,t) = (C_1 e^{-jk_0 z} + C_2 e^{+jk_0 z}) e^{jwt}. \tag{6}$$

The corresponding acoustic particle velocity is

$$u(z,t) = \left(\frac{C_1}{\rho_0 c_0} e^{-jk_0 z} - \frac{C_2}{\rho_0 c_0} e^{+jk_0 z}\right) e^{jwt}. \tag{7}$$

Considering the boundary conditions of point 2 ($z = 0$) and point 1 ($z = \mathrm{L}$), the equation yields

$$\begin{pmatrix} p_2 \\ \rho_0 c_0 u_2 \end{pmatrix} = \begin{bmatrix} 1 & 1 \\ 1 & -1 \end{bmatrix} \begin{pmatrix} C_1 \\ C_2 \end{pmatrix}, \tag{8}$$

$$\begin{pmatrix} p_1 \\ \rho_0 c_0 u_1 \end{pmatrix} = \begin{bmatrix} e^{-jk_0 L} & e^{+jk_0 L} \\ e^{-jk_0 L} & -e^{+jk_0 L} \end{bmatrix} \begin{pmatrix} C_1 \\ C_2 \end{pmatrix}. \tag{9}$$

Combination of Eqs. (8) and (9) results in

$$\begin{pmatrix} p_2 \\ u_2 \end{pmatrix} = \begin{bmatrix} \cos(k_0 L) & jZ_1 \sin(k_0 L) \\ j\frac{1}{Z_1} \sin(k_0 L) & \cos(k_0 L) \end{bmatrix} \begin{pmatrix} p_1 \\ u_1 \end{pmatrix}. \tag{10}$$

Therefore, for a wave propagating normally into a quiescent medium symbolized by "m", the general matrix form between point 1 and point 2 is expressed as

$$\begin{pmatrix} p_2 \\ u_2 \end{pmatrix} = \begin{bmatrix} \cos(k_m L) & jZ_m \sin(k_m L) \\ j\frac{1}{Z_m} \sin(k_m L) & \cos(k_m L) \end{bmatrix} \begin{pmatrix} p_1 \\ u_1 \end{pmatrix}. \tag{11}$$

The absorber's acoustic impedance on the perforated front plate is obtained from the bottom wall of the infinity of impedance [7,12]. The sound absorption mechanism of the single-layer perforated absorber is illustrated in Fig. 2.

As depicted in Fig. 2, there exist four points representing the absorbing impedance within the absorber. The absorber is composed of a structure of "rigid-backing plate $+L$ thickness of air $+D_f$ thickness of the acoustic fiber $+q$ thickness of the perforated front plate". The absorber's acoustic impedance of Z_3 on the perforated front plate is obtained from the acoustically rigid-backing plate of Z_0. As derived in Eq. (11), the relations of acoustic pressure p and acoustic particle velocity u between point 0 and point 1 are expressed as the transfer matrix and

are shown below.

$$\begin{pmatrix} p_1 \\ u_1 \end{pmatrix} = \begin{bmatrix} \cos(\omega L/c_0) & i\rho_0 c_0 \sin(\omega L/c_0) \\ i\frac{\sin(\omega L/c_0)}{\rho_0 c_0} & \cos(\omega L/c_0) \end{bmatrix} \begin{pmatrix} p_0 \\ u_0 \end{pmatrix}. \tag{12}$$

By the development of Eq. (12), it yields

$$Z_1 = -i\rho_0 c_0 \cot\left(\frac{\omega L}{c_0}\right), \tag{13}$$

where p_1 is the acoustic pressure at the surface of the air layer, u_1 is the acoustic particle velocity at the surface of the air layer, p_0 is the acoustic pressure at the absorber's bottom and u_0 is the acoustic particle velocity at the back plate.

The relations of acoustic pressure p and acoustic particle velocity u with respect to point 1 and point 2 are expressed in the transfer matrix below:

$$\begin{pmatrix} p_2 \\ u_2 \end{pmatrix} = \begin{bmatrix} \cos(k_{\text{fiber}} D_f) & jZ_{\text{fiber}} \sin(k_{\text{fiber}} D_f) \\ j\frac{1}{Z_{\text{fiber}}} \sin(k_{\text{fiber}} D_f) & \cos(k_{\text{fiber}} D_f) \end{bmatrix} \begin{pmatrix} p_1 \\ u_1 \end{pmatrix}. \tag{14}$$

By developing Eq. (14), an alternative form of Eq. (14) yields

$$Z_2\left(=\frac{p_2}{u_2}\right) = Z_{\text{fiber}} \frac{Z_1 + jZ_{\text{fiber}} \tan[k_{\text{fiber}} D_f]}{Z_{\text{fiber}} + jZ_1 \tan[k_{\text{fiber}} D_f]} \tag{15a}$$

or

$$Z_2\left(=\frac{p_2}{u_2}\right) = Z_{\text{fiber}} \frac{Z_1 \cosh[k_{\text{fiber}} D_f] + Z_{\text{fiber}} \sinh[k_{\text{fiber}} D_f]}{Z_1 \sinh[k_{\text{fiber}} D_f] + Z_{\text{fiber}} \cosh[k_{\text{fiber}} D_f]}. \tag{15b}$$

For the acoustic impedance between point 1 and point 2, the formula derived in Eq. (15a) is the same as that in Eq. (15b) by Dunn and Davern [6].

By adopting the formula of specific normal impedance and wave number [which is applied in fibrous material and derived by Delany and Bazley [10] at the flow resistivity range R of

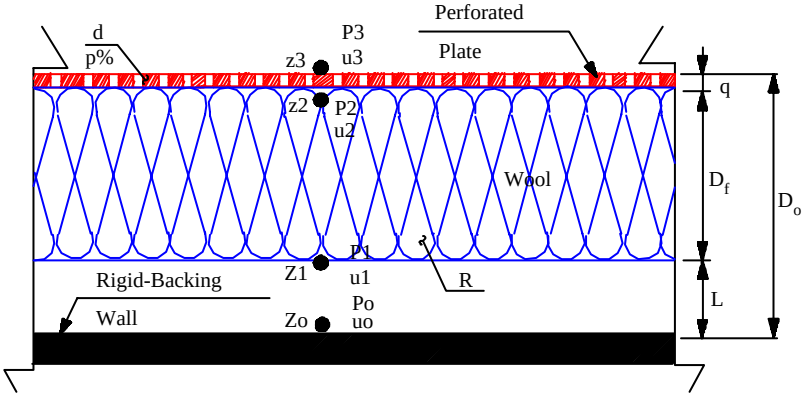

Fig. 2. Sound absorbing mechanism for a single-layer sound absorber.

$10^3 \sim 5 \times 10^4$ (MKS rayls/m)], Eq. (15) can be written as

$$Z_2 = (R_{\text{fiber}} + jX_{\text{fiber}})\left[\frac{\sinh(k_2 D_f)\cos(k_1 D_f) - j\,\sin(k_1 D_f)\cosh(k_2 D_f)}{\cos(k_1 D_f)\cosh(k_2 D_f) - j\,\sinh(k_2 D_f)\sin(k_1 D_f)}\right], \tag{16a}$$

$$k_1 = \frac{\omega}{c_0}\left[1 + c_1\left(\frac{\rho_0 f}{R}\right)^{c_2}\right], \quad k_2 = \frac{\omega}{c_0}\left[c_3\left(\frac{\rho_0 f}{R}\right)^{c_4}\right],$$
$$R_{\text{fiber}} = \rho_0 c_0\left[1 + c_5\left(\frac{\rho_0 f}{R}\right)^{c_6}\right], \quad X_{\text{fiber}} = \rho_0 c_0\left[c_7\left(\frac{\rho_0 f}{R}\right)^{c_8}\right], \tag{16b}$$

where $c_1, c_2, c_3, c_4, c_5, c_6, c_7$ and c_8 are the material constants of the porous acoustic fiber. For the sound flowing into the perforated plate, it is assumed that the incident sound passes through the holes of the perforated plate and is immediately transmitted to the porous material behind the perforated plate; the particle velocity is almost not abated [7,8]. The continuity of the particle velocity is then applied and expressed as

$$u_2 = u_3. \tag{17}$$

By the definition of acoustic impedance, it yields

$$Z_p = \frac{p_3 - p_2}{u_2} \tag{18a}$$

or

$$p_3 = Z_p u_2 + p_2. \tag{18b}$$

Combining Eqs. (17)–(18), the transfer matrix between point 2 and point 3 yields

$$\begin{pmatrix} p_3 \\ u_3 \end{pmatrix} = \begin{bmatrix} 1 & Z_p \\ 0 & 1 \end{bmatrix}\begin{pmatrix} p_2 \\ u_2 \end{pmatrix}. \tag{19}$$

By the development of Eq. (19) and the substitution of Eq. (10), the specific normal impedance at point 3 is in the form

$$Z_3 = Z_2 + Z_p. \tag{20}$$

For a perforated plate backed with the porous material, the resultant impedance at point 3 expressed in Eq. (20) is identical with that derived by Jinkyo et al. [9].

By adopting the formula of specific normal impedance and wave number of the perforated plate from Beranek and Ver [11], one has

$$Z_p = \frac{\rho_0}{\varepsilon}\sqrt{8v\omega}\left(1 + \frac{q}{2d}\right) + j\frac{\omega\rho_0}{\varepsilon}\left[\sqrt{\frac{8v}{\omega}}\left(1 + \frac{q}{2d}\right) + q + \delta\right], \tag{21a}$$

$$\delta = 0.85(2d)\left(1 - 1.47\sqrt{\varepsilon} + 0.47\sqrt{\varepsilon^3}\right). \tag{21b}$$

For normal incidence, the sound absorption coefficient [7–9] is

$$\alpha(f, \varepsilon, d, R, q, D_f, L, D_0) = 1 - \left|\frac{Z_3 - \rho_0 c_0}{Z_3 + \rho_0 c_0}\right|^2 = \alpha(f, p\%, d, R, q, D_f), \tag{22a}$$

$$\text{where } p\% = \varepsilon^* 100, \tag{22b}$$

$$D_0 = D_f + L + q. \tag{22c}$$

3. Case study

The noise control of a machine fan room is introduced as the case in this study. According to the spectrum analysis on sound field, the sound wave at the pure tone of 350 Hz is remarkable.

The thickness of the sound absorber attached onto the wall is required to be less than 0.2 (m) for the necessity of maintenance and operation. To reduce the sound energy at 350 Hz, an attempt for optimal design of the sound absorber is then made under the thickness constraint. An attempt of numerical assessment on shape optimization by using *GA*, *EPFM*, *IPFM*, *FDM* methods is carried out as follows.

4. Model checks

Before performing the *GA* optimal simulation on a single-layer sound absorber, the accuracy check of the mathematical model on the sound absorber is made by experimental data [7,12]. As depicted in Fig. 3, the accuracy comparisons between theoretical and Davern's experimental data for the models reveal that they are in good agreement. Therefore, the proposed fundamental mathematical models are acceptable. Thereafter, the models linked with the numerical method are applied for the shape optimization as explained in the following paragraph.

5. Numerical method

5.1. Gradient method

5.1.1. Sensitivity analysis

To obtain the starting design data, a computer-aided graphic system to judge the sensitivity of the design parameter is thus built and shown in Figs. 4–13. As indicated in Figs. 4–13, the sensitivities of the design parameters at a frequency of 350 Hz are ranked as $D_f = R \geqslant q \geqslant d > p$.

For purpose of lightness, an assumption of the maximal q of 0.01 (m) is thus made prepensely. For the compressibility of acoustic fiber and the availability of material for manufacture three restrictions are specified as

$$D_f \leqslant 0.19(\text{m}); \quad d \leqslant 0.015(\text{m}); \quad p\% \leqslant 50(\%).$$

By using graphical analysis of sensitivities among the above figures, the initial design data for each parameter are thus decided as

$$D_f = 0.05(\text{m}), \ R = 7000\ (\text{rayls/m}), \ d = 0.015(\text{m}), \ p\% = 50(\%), \ q = 0.01(\text{m}).$$

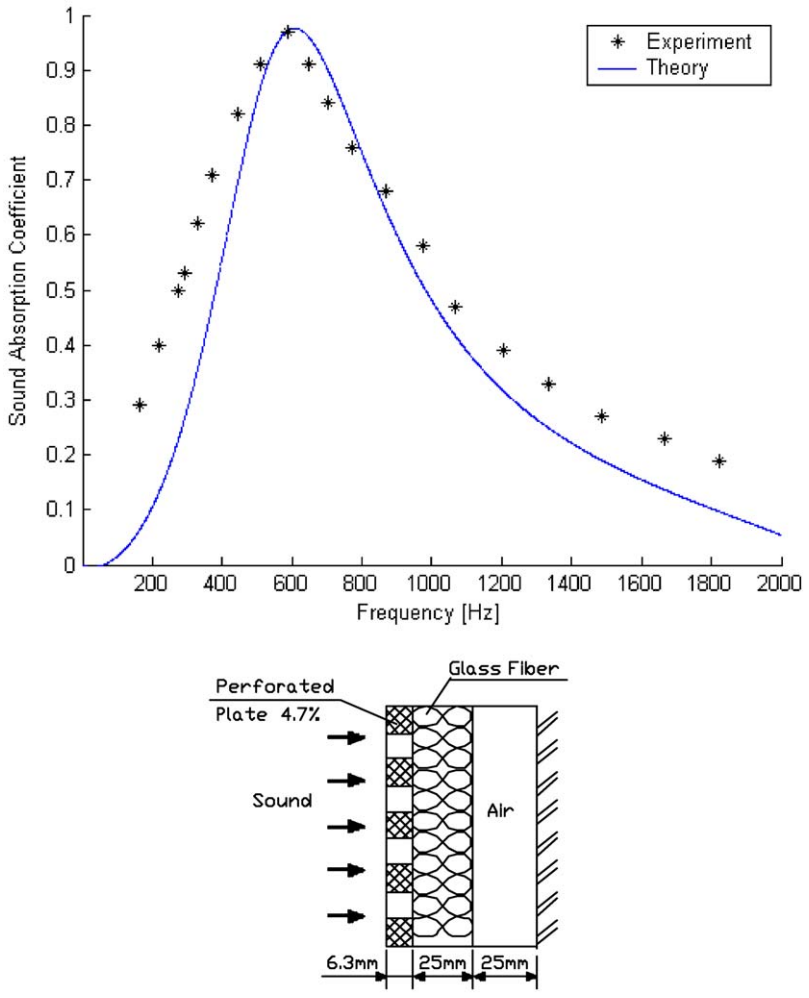

Fig. 3. Performance of a single-layer sound absorber (∗: experimental data [12]).

5.1.2. Mathematical formulation

Minimize $F(X) = -\alpha(X)$ Objective function

Subject to: $g_j(X) \leqslant 0 \;\; j = 1, 3$ inequality constraints

where

$$X = \begin{bmatrix} X_1 \\ X_2 \\ X_3 \\ X_4 \end{bmatrix} = \begin{bmatrix} D_f \\ R \\ d \\ p\% \end{bmatrix} \quad \text{design variable.}$$

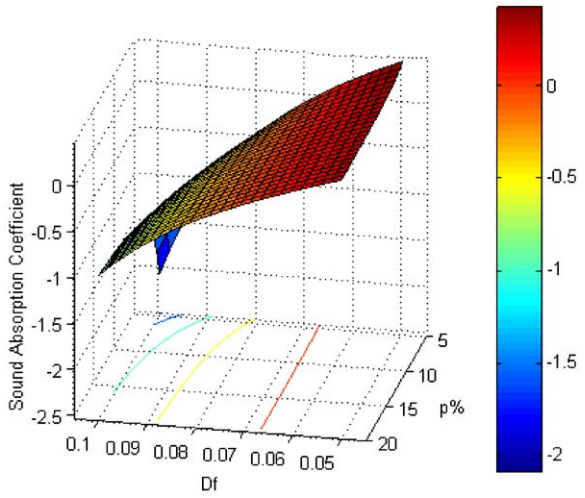

Fig. 4. Performance of α with respect to D_f and $p\%$.

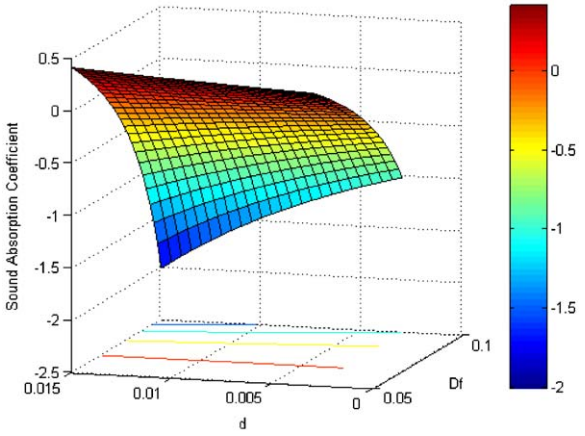

Fig. 5. Performance of α with respect to D_f and d.

To find out the numerical design data, three kinds of searching algorithms (used in the optimal design process) are employed and briefly introduced as follows.

(1)*Exterior penalty function method* (*EPFM*) [1]: The algorithm of exterior penalty function method is shown in Fig. 14. By using exterior penalty function method, Φ is defined by

$$\Phi(X, r_p) = F(X) + r_p \cdot P(X) = F(X) + r_p \sum_{i=1}^{3} \{\max[0, g_i(X)]\}^2,$$

where $g_1 = X_1 - 0.19, \quad g_2 = X_3 - 0.015, \quad g_3 = X_4 - 50.0.$

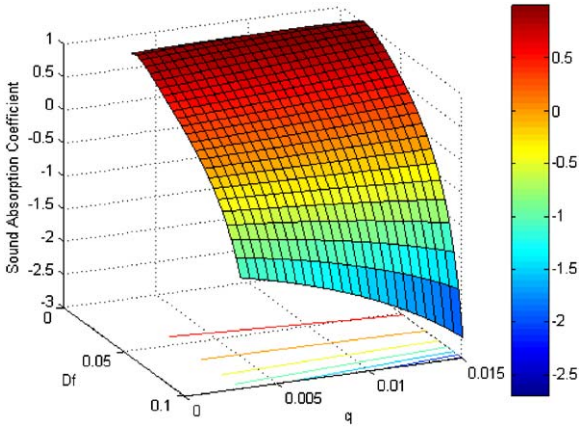

Fig. 6. Performance of α with respect to D_f and q.

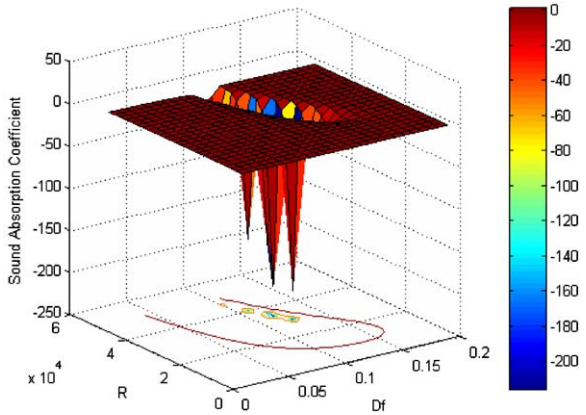

Fig. 7. Performance of α with respect to D_f and R.

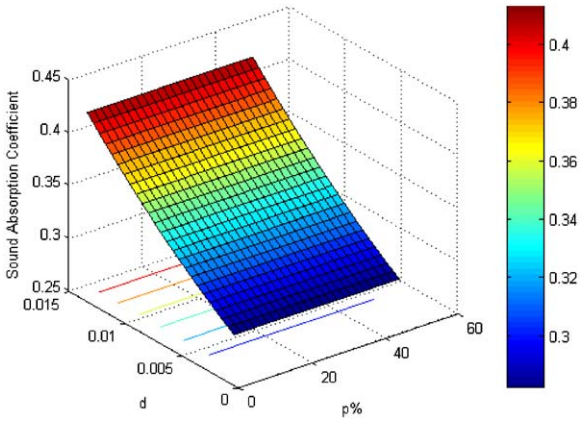

Fig. 8. Performance of α with respect to $p\%$ and d.

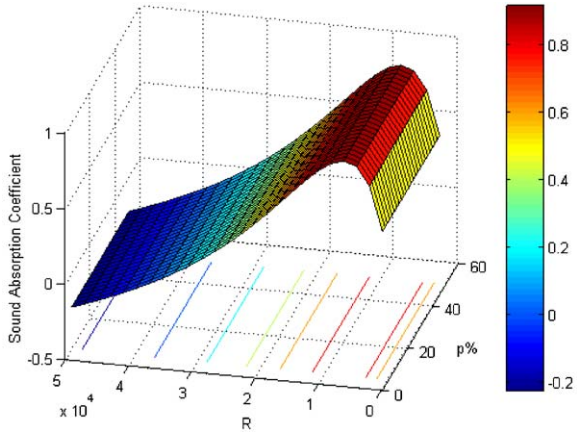

Fig. 9. Performance of α with respect to $p\%$ and R.

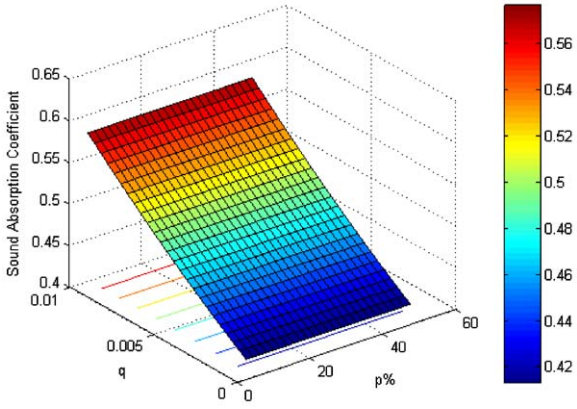

Fig. 10. Performance of α with respect to $p\%$ and q.

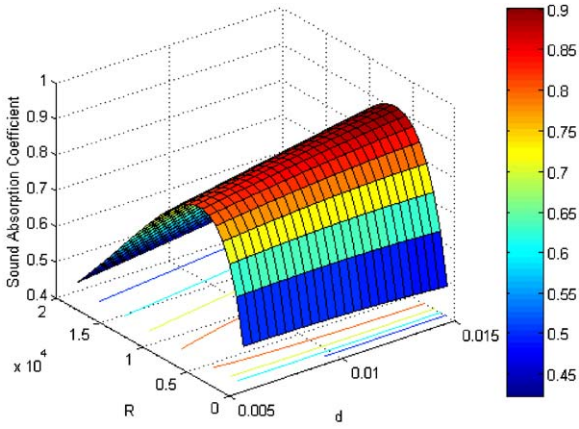

Fig. 11. Performance of α with respect to d and R.

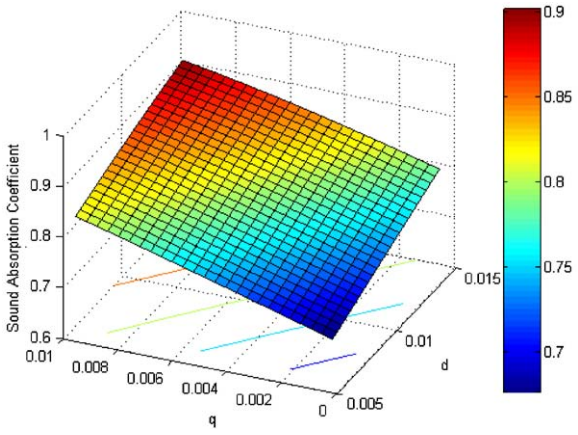

Fig. 12. Performance of α with respect to d and q.

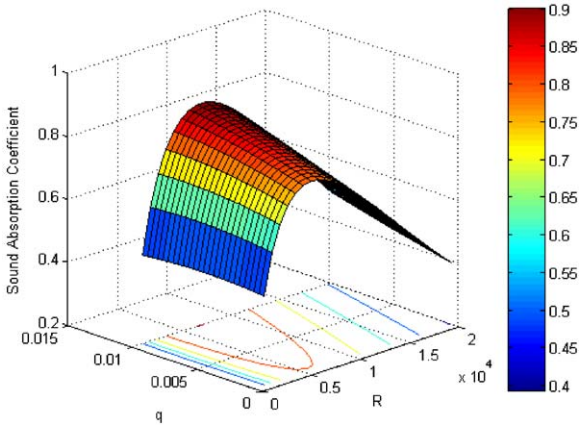

Fig. 13. Performance of α with respect to design parameters of q and R.

(2) *Interior penalty function method* (*IPFM*) [1]: The algorithm of interior penalty function method is shown in Fig. 15. By using interior penalty function method, Φ is defined as

$$\Phi(X, r'_p, r_p) = F(X) + r'_p \sum_{j=1}^{3} \frac{-1}{g_j(X)},$$

where $g_1 = X_1 - 0.19, \quad g_2 = X_3 - 0.015, \quad g_3 = X_4 - 50.0.$

(3)*Feasible direction method* (*FDM*) [1]: The search proceeds from one constraint to another in a zig-zag manner until the optimum is located. The algorithm of feasible direction method is shown in Fig. 16. A tendency of this method is to zig-zag between the constraints.

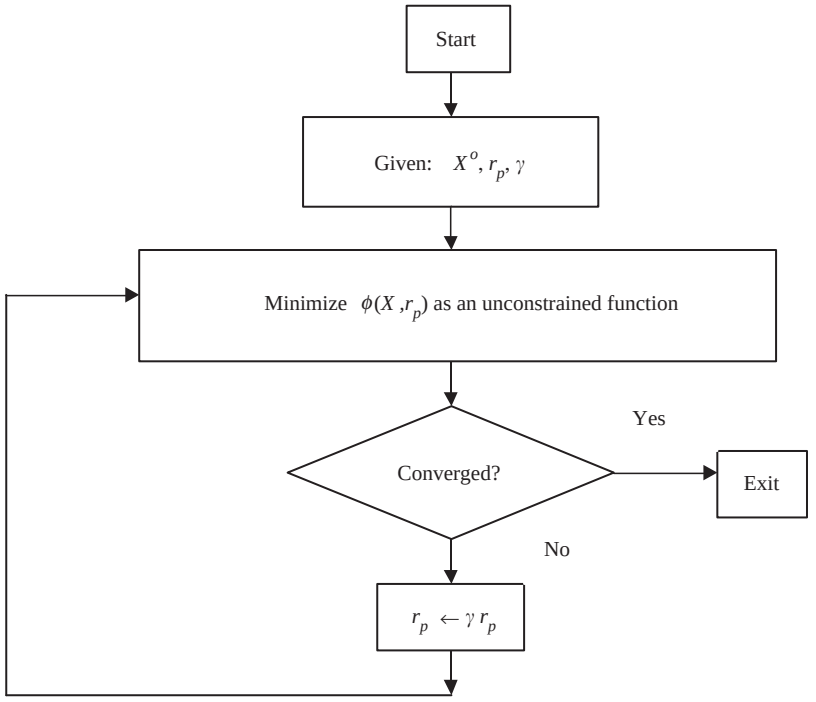

Fig. 14. Algorithm of *EPFM* [1].

5.2. Genetic algorithm

5.2.1. GA elements and scheme

Six kinds of basic elements and schemes included in *GA* are defined as follows.

(1) *Populations and chromosomes*: The initial population is built up by randomization. The parameter set is encoded to form a string, which represents the chromosome. By evaluation of the objective function, each chromosome is assigned with a fitness.

(2) *Parents*: By using the probabilistic computation weighted by the relative fitness, pairs of chromosomes are selected as parents. The weighted roulette wheel selection is then applied. Each individual in the population is assigned space on the roulette wheel, which is proportional to the individual relative fitness. Individuals with the largest portion on the wheel have the greatest probability to be selected as the parent generation for the next generation. A typical selection scheme, a weighted roulette wheel, is depicted in Fig. 17.

(3) *Crossover*: One pair of offspring is generated from the selected parent by crossover. Crossover occurs with a probability of *pc*. Both the random selection of a crossover and combination of the two parent's genetic data are then preceded. The scheme of single-point crossover is chosen in *GA's* optimization. Recombination and parent selection are the principal method for the evolution in *GA*. A typical scheme of single-point crossover is depicted in Fig. 18.

(4) *Mutation*: Genetically, mutation occurs with a probability of *pm* of which the new and unexpected point will be brought into the *GA* optimizer's search domain. It is an essential

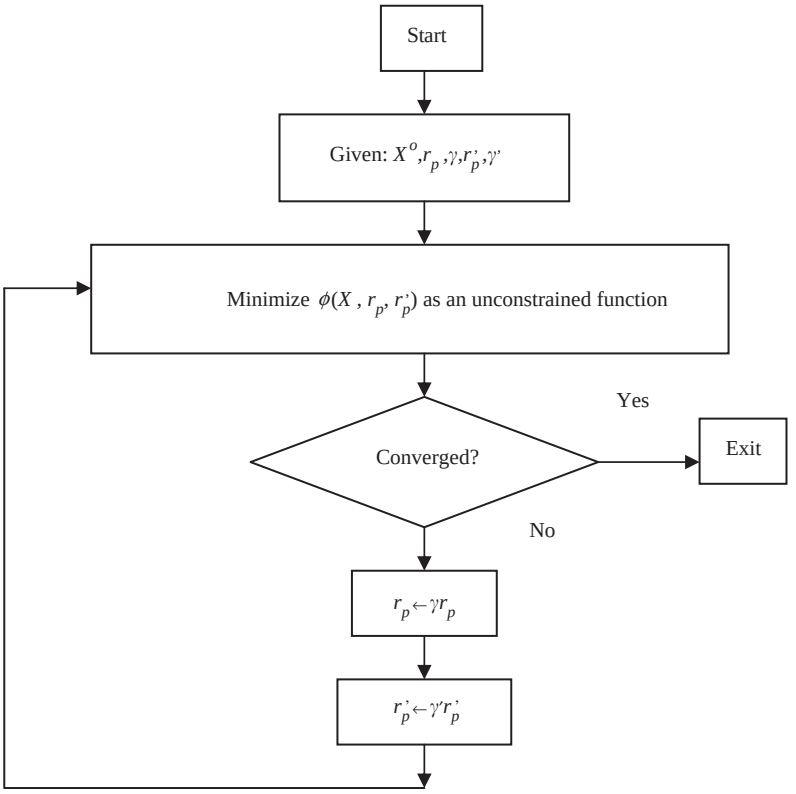

Fig. 15. Algorithm of *IPFM* [1].

operation to improve the accuracy of *GA's* optimization. A typical scheme of mutation is depicted in Fig. 19.

(5) *Elitism*: To prevent the best gene from disappearing and to improve the accuracy of optimization during reproduction, the elitism scheme to keep the best gene in the parent generation is thus presented and developed.

(6)*New generation*: Reproduction includes selection, crossover, mutation, and elitism. The reduplication continues until a new generation is constructed and the original generation is substituted. Highly fit characteristics produce more copies of themselves in the subsequent generation resulting in a movement of the population toward an optimal direction. The process can be terminated when number of generations exceeds a pre-selected value.

The operations in *GA* method are pictured in Fig. 20. The block diagram of *GA* optimization on the single-layer sound absorber is depicted in Fig. 21.

(*B*) *GA parameters*: The number of the population (*popuSize*) is set as 60. The maximum generation (*gen_no*) is set as 500. The bit length (*bit_no*) is set as 40. To achieve a better approach in *GA*, the investigation of *GA* parameters (*pc*, *pm* and *elit*) by varying these parameters in order is thus proceeded and discussed. As described by Johnson and Yahya [13], one set of *GA* parameters of *pc*, *pm* and *elit* is chosen as 0.8, 0.05 and 1 individually. The variables in *GA* include the D_f, $p\%$,

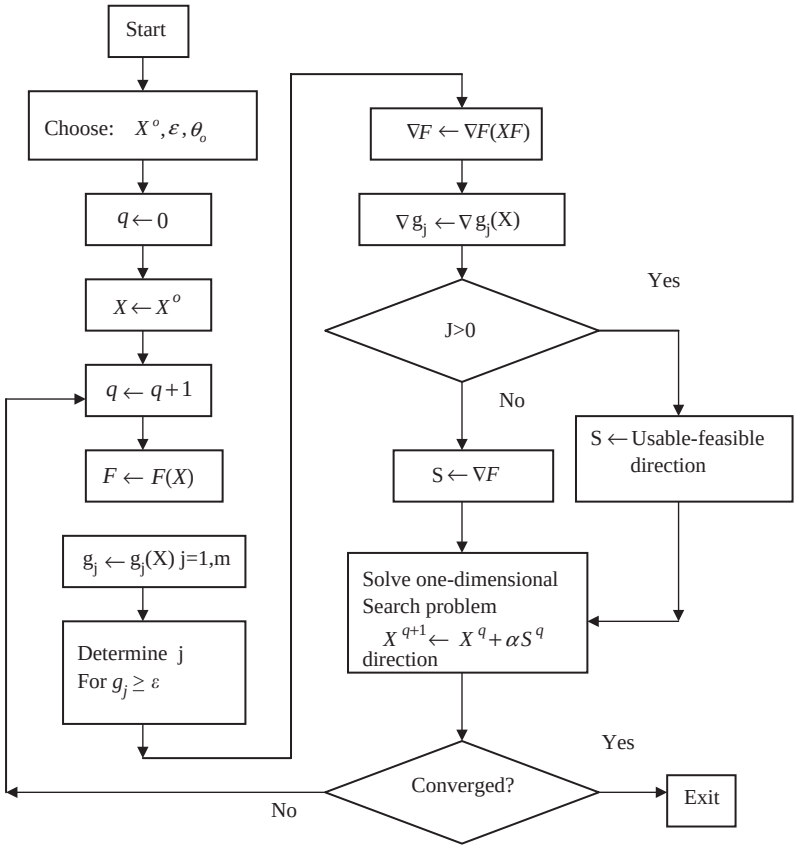

Fig. 16. Algorithm of *FDM* [1].

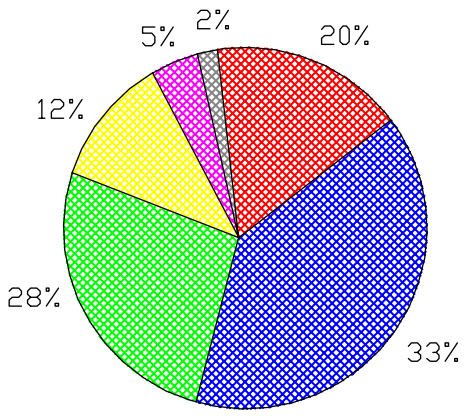

Fig. 17. Weighted roulette wheel method of selection.

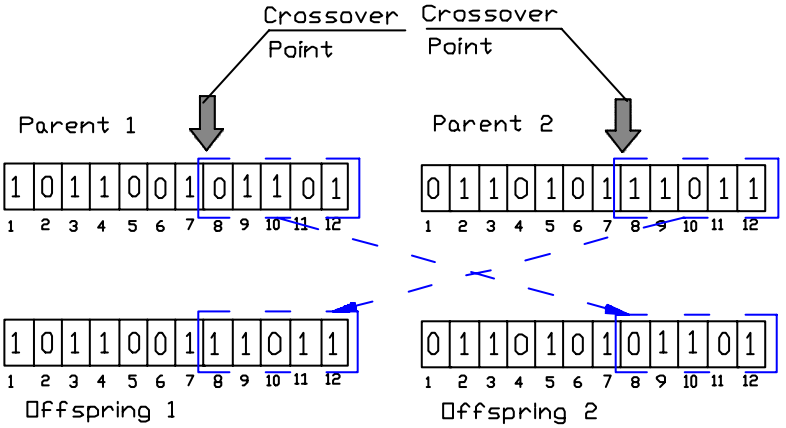

Fig. 18. Scheme of single-point crossover.

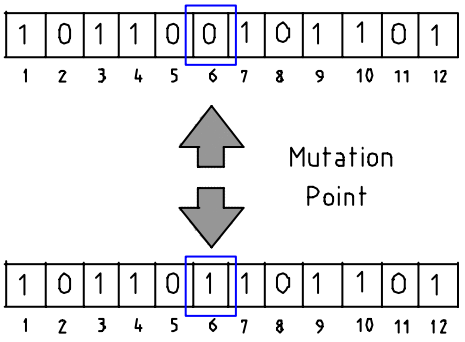

Fig. 19. Scheme of mutation.

d and R. The corresponding data constraints for the above variables are [0 0.19], [5 50], [0.003 0.015] and [1000 50000] individually.

6. Results and discussion

6.1. Results

6.1.1. Mathematical optimal searching techniques

The optimal results by *EPFM*, *IPFM* and *FDM* are summarized in Table 1. As indicated in Table 1, it reveals that *EPFM* shows a better result of sound absorption coefficient at the design frequency of 350 Hz. By using these design data in the calculation, the sound absorption coefficients with respect to frequency are plotted in Fig. 22. As indicated in Fig. 22, the sound absorption coefficient at the concerned frequency of 350 Hz is maximized in each scheme. The accuracy check of these results by using the Kuhn–Tucker condition [1] is performed and

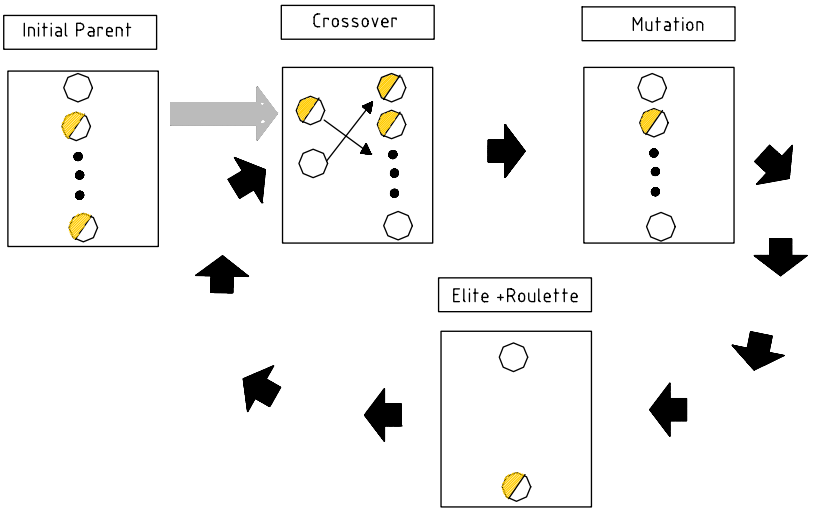

Fig. 20. Operations in *GA* method.

summarized in Table 2. As indicated in Table 2, it reveals that *EPFM* is much closer to the accuracy criteria.

6.1.2. GA method

To obtain the optimal design value of sound absorption (α) on sound absorber, four sets of *GA* parameters are being tried. The analyses are summarized in Table 3 and plotted in Fig. 23. According to Table 3, the better result in the first case ($pc = 0.8$; $pm = 0.05$; $elit = 1$) of *GA* set is found.

6.2. Discussion

By using the design data of *EPFM*, *IPEM*, *FDM* and *GA* ($pc = 0.8$; $pm = 0.05$; $elit = 1$) in the calculation and plot, a comparison chart in them are made and plotted in Fig. 24. As shown in Fig. 24, it proves that both of *EPFM* and *GA* have the better results.

7. Conclusion

It has been shown that both GA method and classical mathematical searching can be used in the optimization of a single-layer sound absorber by adjusting both the absorber's shape and absorbing material under the space constraints. Because no need of sensitivity analyses for choosing the starting design data, which is required in classical methods of *EPFM*, *IPFM* and *FDM*, are necessary *GA* becomes easier to use. In addition, the *GA*'s accuracy can be improved when all the *GA* parameters of crossover, mutation and elitism are taken into consideration

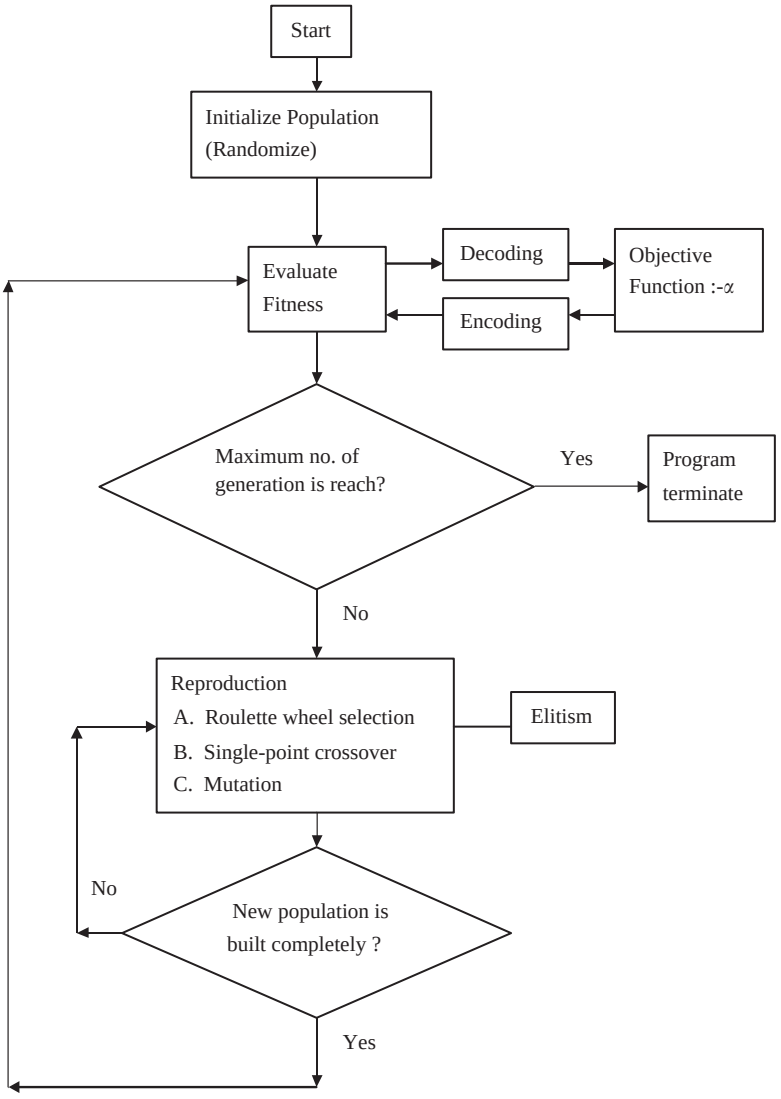

Fig. 21. Block diagram of the *GA* optimization.

Table 1
Optimal sound absorption coefficient with respect to the optimal design parameters in three methods

	D_f	R	d	$p\%$	α
Exterior penalty function method	0.036	17459	0.0019	4.6	0.999998
Interior penalty function method	0.050	7000	0.015	15	0.870331
Feasible direction method	0.038	7563	0.015	14.9	0.879046

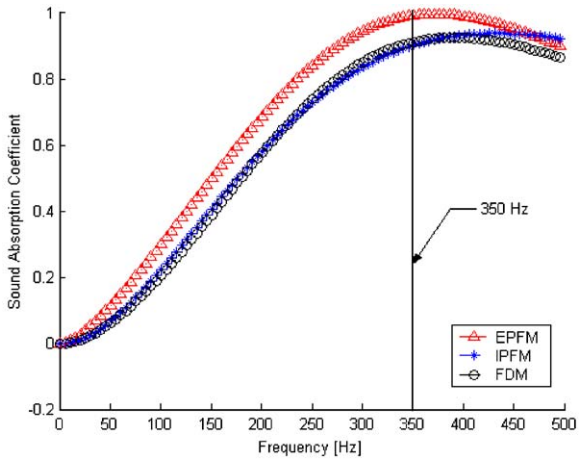

Fig. 22. Optimal profiles in classical mathematical searching.

Table 2
Results of Kuhn–Tucker condition's checking process in three methods

	Lagrange multipliers			Residual vector			
	λ_1	λ_2	λ_3	$\{R_1\}$	$\{R_2\}$	$\{R_3\}$	$\{R_4\}$
Exterior penalty function method (*EPFM*)	0.0091	0.024	0.016	0.0	−.29E−02	−.18E−08	0.0
Interior penalty function method (*IPFM*)	−0.117	0.506	−0.135	0.0	−.12E+00	0.0	.15E−07
Feasible direction method (*FDM*)	0.172	0.264	−0.077	0.0	−.23E+00	0.0	0.0

Table 3
Comparison of results for the variations of control parameters

Common parameters			Control parameters			Results				
popuSize	*gen_no*	*bit_no*	*pc*	*pm*	*elt_no*	*p*%	*R*	*d*	D_f	α
60	500	40	0.8	0.05	0	24.7	39673	0.0105	0.1286	0.999943
60	500	40	0.8	0.05	1	31.8	48168	0.0043	0.1150	0.999936
60	500	40	0.8	0	1	17.7	28816	0.0108	0.1493	0.999543
60	500	40	0	0.05	1	37.1	28483	0.0074	0.1142	0.999938

simultaneously. Besides, the accuracy check of classical gradient schemes by the Kuhn–Tucker condition [1] indicates that the solution of *EPFM* is acceptable. Therefore, there exist two better sets of design data by *GA* and *EPFM* to increase the ability of sound absorption.

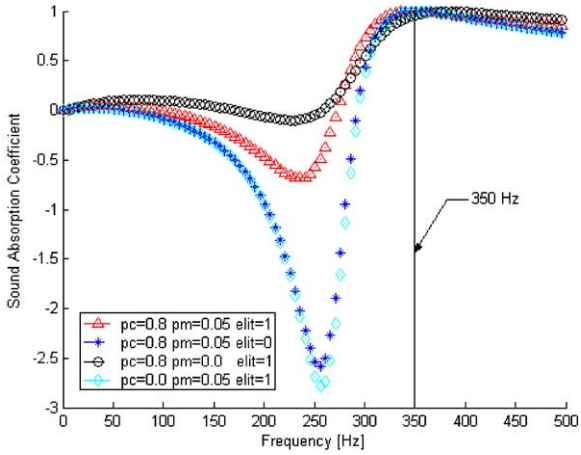

Fig. 23. Sound absorption coefficient with respect to *GA* parameters-crossover (*pc*), mutation (*pm*) and elitism (*elit*).

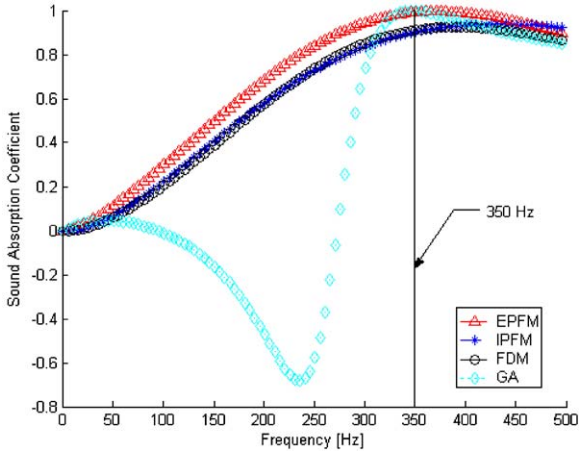

Fig. 24. Optimal profiles in *EPFM*, *IPFM*, *FDM* and *GA*($pc = 0.8$; $pm = 0.05$; $elit = 1$).

Acknowledgements

The authors would like to thank the reviewer for helpful advice in the text.

References

[1] Vanderplaats, N. Garret, *Numerical Optimization Techniques for Engineering Design: With Applications*, McGraw-Hill, New York, 1984.

[2] K. Weeber, S. Ratnajeevan, H. Hoole, Geometric parametrization and constrained optimization techniques in the design of salient pole synchronous machines, *IEEE Transaction on Magnetics* 28 (4) (1992) 1948–1960.

[3] G.V. Reklaitis, A. Ravindran, K.M. Ragsdell, *Engineering Optimization: Method and Applications*, Wiley, New York, 1984.
[4] D.E. Goldberg, *Genetic Algorithm in Search, Optimization and Machine Learning*, Addison-Wesley, Massachusets, 1988.
[5] M.C. Chiu, Compact acoustic board for low frequencies: experimental study and theoretical analysis, *Proceedings of the 18th National Conference on Mechanical Engineering, CSME C3*, 2001, pp. 719–724.
[6] I.P. Dunn, W.A. Davern, Calculation of acoustic impedance of multi-layer absorbers, *Applied Acoustics* 19 (1986) 321–334.
[7] F.C. Lee, W.H. Chen, Acoustic transmission analysis of multi-layer absorbers, *Journal of Sound and Vibration* 248 (2001) 621–634.
[8] M.L. Munjal, *Acoustics of Ducts and Mufflers with Application to Exhaust and Ventilation System Design*, Wiley, New York, 1987.
[9] L. Jinkyo, W. George, J. Swenson, Compact sound absorbers for low frequencies, *Noise Control Engineering Journal* 38 (1992) 109–117.
[10] M.E. Delany, E.N. Bazley, Acoustical properties of fibrous absorbent materials, *Applied Acoustics* 13 (1969) 105–116.
[11] L.L. Beranek, I.L. Ver, *Noise and Vibration Control Engineering*, Wiley, New York, 1992 pp. 232–243 (Chapter 8).
[12] W.A. Davern, Perforated facings backed with porous materials as sound absorbers—an experimental study, *Applied Acoustics* 10 (1977) 85–112.
[13] J.M. Johnson, R.S. Yahya, Genetic algorithm optimization and its application to antenna design, *Proceedings of the IEEE Antennas and Propagation Society International Symposium*, 1994, pp. 326–331.